6044 *Biochemistry* **2009,** *48,* 6044–6051
DOI: 10.1021/bi900236k

BIOCHEMISTRY
including biophysical chemistry & molecular biology
Article

Competitive Inhibition of Human Poly(A)-Specific Ribonuclease (PARN) by Synthetic Fluoro-Pyranosyl Nucleosides†

Nikolaos A. A. Balatsos,[‡,∥] Dimitrios Vlachakis,[§] Panagiotis Maragozidis,[‡] Stella Manta,[‡] Dimitrios Anastasakis,[‡] Athanasios Kyritsis,[‡] Metaxia Vlassi,[§] Dimitri Komiotis,[‡] and Constantinos Stathopoulos*[,‡,∥]

[‡]*Department of Biochemistry & Biotechnology, University of Thessaly, 26 Ploutonos Street, 412 21 Larissa, Greece,* [§]*Institute of Biology, National Centre for Scientific Research "Demokritos", 153 10 Aghia Paraskevi, Attikis, Greece, and* [∥]*Institute of Biomedical Research & Technology (BIOMED), 51 Papanastasiou Street, 412 22 Larissa, Greece*

Received February 13, 2009; Revised Manuscript Received May 14, 2009

ABSTRACT: Poly(A)-specific ribonuclease (PARN) is a cap-interacting deadenylase that mediates, together with other exonucleases, the eukaryotic mRNA turnover and thus is actively involved in the regulation of gene expression. Aminoglycosides and natural nucleotides are the only reported modulators of human PARN activity, so far. In the present study, we show that synthetic nucleoside analogues bearing a fluoro-glucopyranosyl sugar moiety and benzoyl-modified cytosine or adenine as a base can effectively inhibit human PARN. Such nucleoside analogues exhibited substantial inhibitory effects, when tested against various cancer cell lines, as has been previously reported. Kinetic analysis showed that the inhibition of PARN is competitive and could not be released by altering Mg(II) concentration. Moreover, substitution of the 2′, 4′, or 6′-OH of the sugar moiety with acetyl and/or trityl groups was crucial for inhibitory efficacy. To understand how the nucleosides fit into the active site of PARN, we performed molecular docking experiments followed by molecular dynamics simulations. The *in silico* analysis showed that these compounds can efficiently dock into the active site of PARN. Our results support the idea that the sugar moiety mediates the stabilization of the nucleoside into the active site through interactions with catalytic amino acid residues. Taken together, our *in vitro* and *in silico* data suggest that human PARN is among the molecular targets of these compounds and could act therapeutically by lowering the mRNA turnover rate, thus explaining their known *in vivo* inhibitory effect at the molecular level.

Deadenylases are Mg(II)-dependent exoribonucleases that constantly degrade poly(A) tails, releasing 5′-AMP [for a recent review, see ref (*1*)]. Among all deadenylases, poly(A)-specific ribonuclease (PARN[1]) is unique since it interacts both with the 5′-cap structure and the poly(A) tail during deadenylation (*2*−*5*). The enzyme is located both in the nucleus and in the cytoplasm of eukaryotic cells (*6*). Biochemical studies have shown that Mg(II) ions are necessary for catalysis, although no such ions were found in the crystal structure of a truncated form of the enzyme (*7*, *8*). PARN activity is modulated *in vitro* through interactions with auxiliary protein factors, as well as with the 5′ cap (*3*, *9*−*16*). PARN is an important mediator of mRNA turnover in eukaryotes and regulates in-part gene expression. In particular, when abnormal cell proliferation requires up-regulation of translation levels and mRNA recycling, PARN could represent a potential molecular target for compounds that suppress the rate of these processes. However, there are limited reports on inhibitors of PARN that could modulate the enzyme's activity. It is known that human PARN can be inhibited by aminoglycosides, where the compounds are proposed to distort the active site and/or displace functionally important divalent ions, such as Mg(II). Aminoglycosides are antibiotics widely used in clinical practice and this inhibition could explain the toxicity side effects that these antibiotics exhibit during treatment (*17*). Furthermore, it has been shown that natural purine nucleotides also inhibit PARN activity (*18*, *19*). More specifically, we have shown previously that RTP nucleotides inhibit the enzyme noncompetitively, while RDP and RMP act in a competitive manner (*19*).

Nucleoside analogues have been widely used against cancer and viral infections (*20*). A common strategy for designing novel nucleoside analogues is the modification of the sugar moiety. For instance, araC and gemcitabine are sugar-modified cytosine analogues. AraC inhibits DNA polymerization and has been used in the clinic against acute myeloblastic leukemia (*21*), while gemcitabine (dFdC) bearing a fluoro-modified sugar that was initially designed as an antiviral agent has been shown to inhibit DNA synthesis, ribonuclease reductase, and incorporate into RNA (*22*, *23*). In addition, several nucleoside analogues are in front-line treatment of diseases caused by RNA viruses (*24*, *25*). All these compounds are metabolized primarily to endogenous

†This work was supported in part by a Research Grant from the University of Thessaly Research Committee (to N.B. and C.S.). A.K. is a recipient of a postgraduate fellowship from Bodossaki Foundation, which is gratefully acknowledged.

*To whom correspondence should be addressed. Tel: +30-2410-565278. Fax: +30-2410-565290. E-mail: cstath@bio.uth.gr.

[1]Abbreviations: PARN, poly(A)-specific ribonuclease; RTP, RDP, RMP, purine nucleotide tri-, di-, monophosphate, respectively; rmsd, root-mean-square deviation; Bz, benzoyl.

 Published on Web 05/27/2009

nucleotides and nucleosides, and the active metabolites target one or more enzymes, such as DNA and RNA polymerases. Ribonuclease activities could also represent potential molecular targets for inhibition by nucleoside analogues. Such is the case of the RNase H domain of HIV RNA-dependent DNA polymerase (*26*−*28*).

During recent years, nucleoside analogues with a six-membered carbohydrate moiety, such as ketonucleosides, have been evaluated for their anticancer and antiviral potential (*29*−*32*). Furthermore, the addition of a fluorine atom on the sugar ring and the addition of a benzoyl-group on the base improves the biological activity of the analogue (ref (*31*) and references therein). However, no molecular target of these compounds or their synthetic intermediates has been identified so far. The above-mentioned work, prompted us to study human PARN as a potential molecular target for inhibition by such nucleoside analogues. We focused on this enzyme given that its activity is reduced by natural nucleotides, its structure is known to a significant extent, and it exhibits the major deadenylation activity in mammals. We demonstrate that PARN can be efficiently inhibited by several nucleoside analogues bearing a six-membered fluoro-modified sugar moiety with or without the benzoyl group on the base (adenine or cytosine). We find that these analogues behave as competitive inhibitors of PARN and more importantly, increased magnesium(II) ion concentrations could not restore the enzyme's activity. To support our biochemical data, we performed molecular docking experiments followed by molecular dynamics (MD) simulations, and we predicted the docking conformation of the nucleosides into the active site. Both the biochemical and the *in-silico* 3D-model analyses revealed a crucial role of the three hydroxyl groups of the sugar moiety for efficient inhibitory effect. Our data suggest that the analogues used in the present study could serve as lead compounds for the development of novel inhibitors of PARN and possibly other essential deadenylases with potential use for novel therapeutic approaches.

MATERIALS AND METHODS

Materials. All chemicals including purine ribonucleotides and deoxynucleotides, methylene blue, and polyadenylic acid potassium salt (average size 300 adenosines, A_{300}) were from SigmaAldrich.

Synthesis of Nucleosides Analogues. The fluoro-pyranosyl nucleosides were synthesized as previously described (*31*). Briefly, condensation of 1,2,4,6-tetra-*O*-acetyl-3-deoxy-3-fluoro-glucopyranose with cytosine, silyated N^4-benzoyl cytosine, or N^6-benzoyl adenine resulted in the production of [1-(2′,4′,6′-tri-*O*-acetyl-3′-deoxy-3′-fluoro-β-D-glucopyranosyl)-N^4-benzoyl cytosine] (A5) or [9-(2′,4′,6′-tri-*O*-acetyl-3′-deoxy-3′-fluoro-β-D-glucopyranosyl)-N^6-benzoyl adenine] (A1), respectively, in the presence of trimethylsilyl trifluoromethane-sulfonate and tin chloride. Deprotection of A5 and A1 with NaOH-ethanol-pyridine yielded [1-(3′,4′-dideoxy-3′-fluoro-β-D-glucopyranosyl)] cytosine (C6), [1-(3′,4′-dideoxy-3′-fluoro-β-D-glucopyranosyl)-N^4-benzoyl cytosine] (A6), or [9-(3′,4′-dideoxy-3′-fluoro-β-D-glucopyranosyl)-N^6-benzoyl adenine] (A2), respectively. Treatment of A2 with 2,2-dimethoxypropane in dry *N*,*N*-dimethylformamide, followed by acetylation of the free hydroxyl group in the 2′ position of the sugar moiety with acetic anhydride/pyridine, removal of the isopropylidene group, and, finally, selective protection of the primary 6′-hydroxyl group with a trityl group yielded compound A4. Oxidation of the fluoro acetylated precursor A4 with pyridinium dichromate/acetic anhydride afforded [9-(3′-deoxy-3′-fluoro-6′-*O*-trityl-β-D-*glycero*-hex-2′-enopyranosyl-4′-ulose)-N^6-benzoyl adenine (A3).

Expression and Purification of Recombinant PARN. The plasmid encoding full-size 74 kDa human PARN (kindly provided by Prof. A. Virtanen, Uppsala University, Sweden) (for expression of N-terminal His_6-tagged polypeptide) was transformed into BL21(DE3) cells to express the recombinant protein as described previously (*33*) with some modifications. Briefly, colonies were grown overnight at 37 °C in the presence of kanamycin (50 μg/mL). The cultures were then diluted (1:100) in the same medium and grown at 37 °C induced by isopropyl-1-thio-β-D-galactopyranoside (IPTG) at a final concentration of 0.1 mM. Cultures for PARN expression were allowed to grow for 3 h at 37 °C. Cells were harvested by centrifugation for 20 min at 4 °C, and pellets were frozen at −70 °C. The expressed His-tagged soluble proteins were purified following previously described protocols (*33*).

PARN Activity Assay and Kinetic Analysis. The enzymatic activity was determined by the methylene blue assay as described before (*34*). Deadenylation rates as a function of time were determined with time-course assays (Supporting Information, Figure S1). Methylene blue buffer was prepared by dissolving 1.2 mg of methylene blue into 100 mL of MOPS buffer (0.1 M MOPS-KOH, pH 7.5, and 2 mM EDTA). The standard reaction buffer contained 20 mM HEPES-KOH (pH 7.0), 1.5 mM $MgCl_2$, 100 mM KCl, 0.1 U of RNasin, 0.2 mM EDTA, 0.25 mM DTT, 10% (v/v) glycerol, and 0.075−0.6 mM of poly(A). All ribonucleotides were dissolved in reaction buffer prior to use. The reactions were performed using 0.01−0.02 mM recombinant PARN. For kinetic analysis, the substrate concentration [poly (A)] varied from 0.075 to 0.6 mM (*19*). The final reaction volume was 100 μL, and the reaction was performed at 30 °C for 5−10 min. The reaction was terminated by mixing the reaction solution with 900 μL of methylene blue buffer, and the mixed solution was incubated at 30 °C for another 15 min in the dark in a water bath. The absorbance at 662 nm of 1 mL of sample was measured on a Spectronic Genesys 20 spectrophotometer.

Coordinate Preparation. The coordinates of PARN were obtained from the known PARN crystal structure as deposited with the RCSB Protein databank (RCSB code: 2A1R). One of the two identical active sites of the dimeric form was used for the docking calculations. All crystallographic water molecules were removed from the coordinate file prior to docking. Hydrogen atoms and partial charges were added to the enzyme by the molecular operating environment (MOE) program (*35*) using the AMBER94 forcefield. MOE used the PEOE method to assign partial charges for all potential inhibitor compounds. After all non-hydrogen atoms were fixed, the PARN molecule was energetically minimized by a combination of the steepest descent, conjugate gradient, and truncated Newton minimization methods within MOE. Energy minimizations were also performed to relax the substrates prior to docking.

Molecular Docking. The MOE suite was used to perform docking experiments and calculations of solvation and relative binding free energies. The Dock module of MOE utilizes a Monte Carlo simulated annealing (SA) method in docking calculations. A docking box of 60 × 40 × 40 points with a grid spacing of 0.375 Å was placed around the active site of the protein for this purpose. The iteration limit was set to 20000, the number of cycles was set to 20, and the number of runs was set to 10.

Molecular Dynamics Simulations. Molecular Dynamics (MD) simulations were performed using MOE and its built-in MD module using an NVT ensemble (N, number of atoms; V, volume; T, temperature). The complexes of the enzyme with the

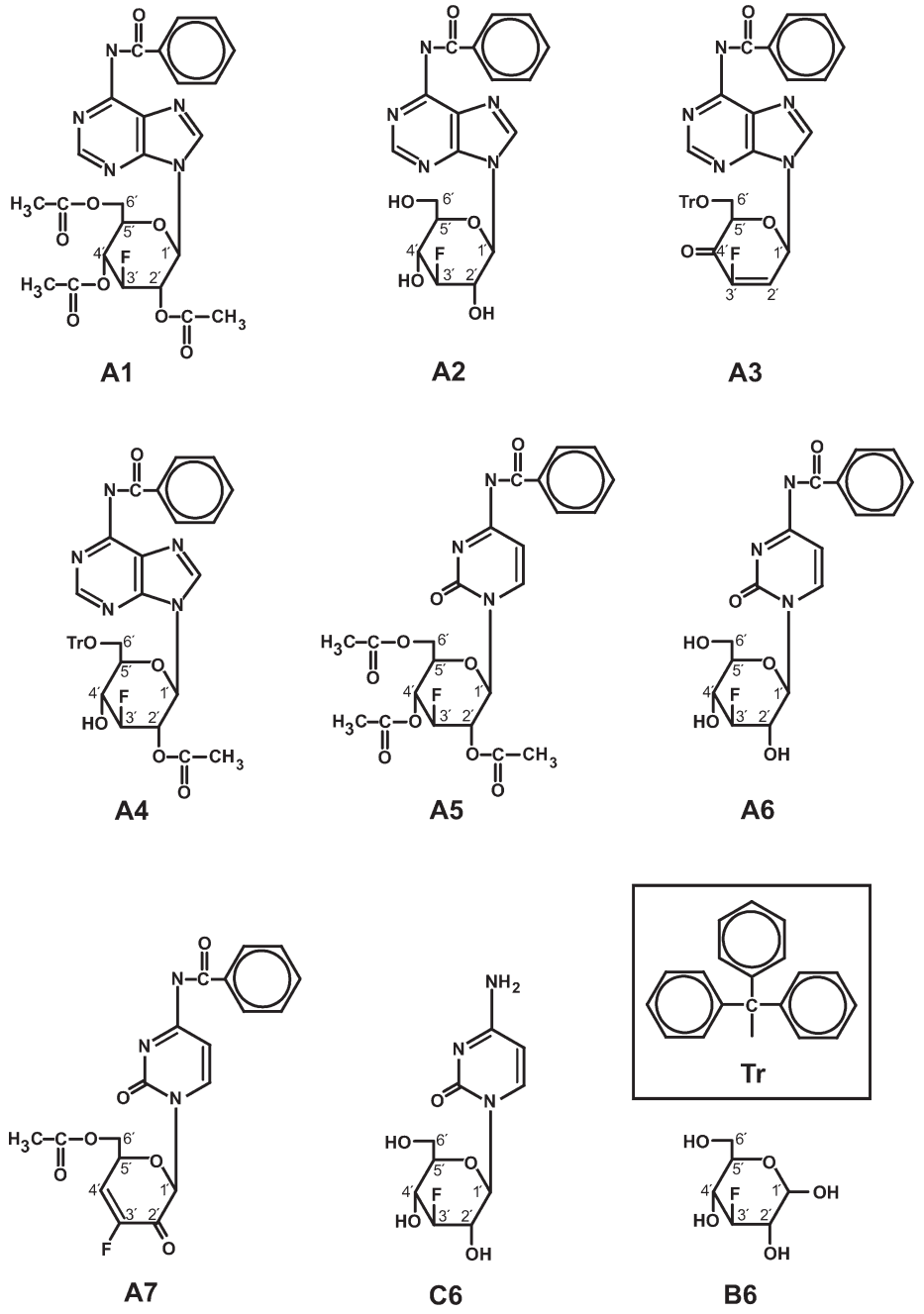

FIGURE 1: Structural formulas of the synthetic nucleosides used.

docked compounds were initially optimized by energy minimization using the AMBER94 force field of MOE. Each complex was subsequently solvated in a periodic box of explicit water molecules extending 8−12 Å from the protein atoms. Periodic boundaries were used in order to minimize edge effects. The water structure was first equilibrated for 100 ps keeping the whole protein fixed followed by a 100 ps equilibration with fixed the protein backbone. The equilibration phase was followed by a 3 ns MD simulation at 300 K with a time step for integration of the potential function of 2 fs. A nonbonded cutoff of at least 8 Å was used.

RESULTS

A2, A6, and C6 Are Competitive Inhibitors of PARN Activity. On the basis of our previous studies showing that AMP, one of the deadenylation products, behaves as a competitive inhibitor of PARN (*19*), we searched for inhibitors of similar chemical nature. We examined the effect of a series of fluoro-pyranosyl nucleosides as potential inhibitors (Figure 1). It has been recently demonstrated that some of these compounds exhibit tumor-inhibitory effects, as well as antiviral activity in cell cultures (*31*). Preliminary screening on the effect of these nucleosides on PARN activity showed that A2, A6, and C6 could efficiently inhibit PARN, while compounds A1, A3−A5, and A7 have no significant effect (data not shown). In order to further characterize the inhibitory effect of A2, A6, and C6 nucleoside analogues, we performed detailed kinetic analysis, which revealed that these compounds behave as efficient competitive inhibitors of PARN *in vitro*. Subsequently, from the kinetic analysis we determined the inhibition constants (K_i shown as inset in Figure 2) for the three compounds. For A2, the calculated K_i value was 0.51 mM, and for A6, K_i was 0.21 mM (Table 1, Figure 2). The same kinetic analysis was performed for the fluoro-pyranosyl

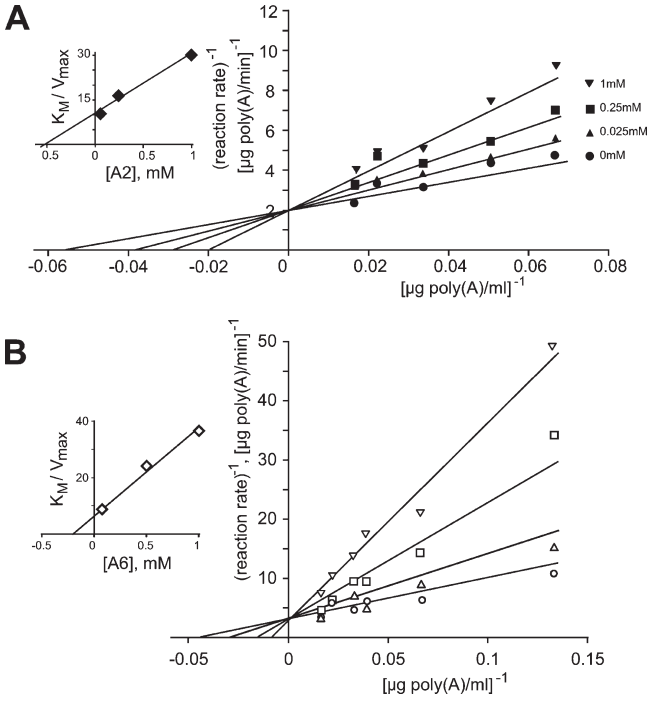

FIGURE 2: Benzoyl fluoro-pyranosyl nucleosides inhibit PARN activity: A2 and A6 are noncompetitive inhibitors. Double reciprocal plots $1/v$ versus 1/[substrate] for PARN activity in the presence of A2 (A) or A6 (B) are shown. The A2 concentrations (filled markers in A) were 0 mM (circle), 0.025 mM (triangle), 0.25 mM (square), and 1 mM (inverted triangle). A6 concentrations (empty markers in B) were 0 mM (circle), 0.05 mM (triangle), 0.5 mM (square), and 1 mM (inverted triangle). Representative plots of at least three independent experiments are shown. Insets: slopes (K_M/V_{max}) of the double reciprocal lines versus the nucleotide concentrations.

Table 1: Inhibition Constants of the Compounds Used in the Present Study

	K_i, μM
A2	510 ± 52
A6	210 ± 45
C6	645 ± 37
CMP	710 ± 105
AMP[a]	1600 ± 348

[a] From ref (*19*).

nucleoside with a cytosine lacking the benzoyl modification (C6), which could also inhibit PARN activity (Figure 3A) with a K_i of 0.6 mM. 3-Deoxy-3-fluoro-glucopyranose (B6), which contains only the same sugar ring without the base moiety, showed no inhibition and in subsequent analysis was used as a negative control (data not shown). Additionally, we compared the inhibitory effect of these compounds with the natural nucleotide CMP that behaved as a competitive inhibitor. The calculated K_i for CMP was 0.7 mM (Figure 3B), similar to that of C6, but higher than that of A6. Table 1 summarizes all of the inhibitory constants of the compounds used in the study. These results show that PARN can be effectively inhibited by the synthetic nucleosides that were tested in the present study, in a competitive manner and imply that this inhibition depends more on the nature of the sugar moiety than on the nature of the base. Furthermore, our data suggest that PARN could represent a novel molecular target of these compounds *in vitro*.

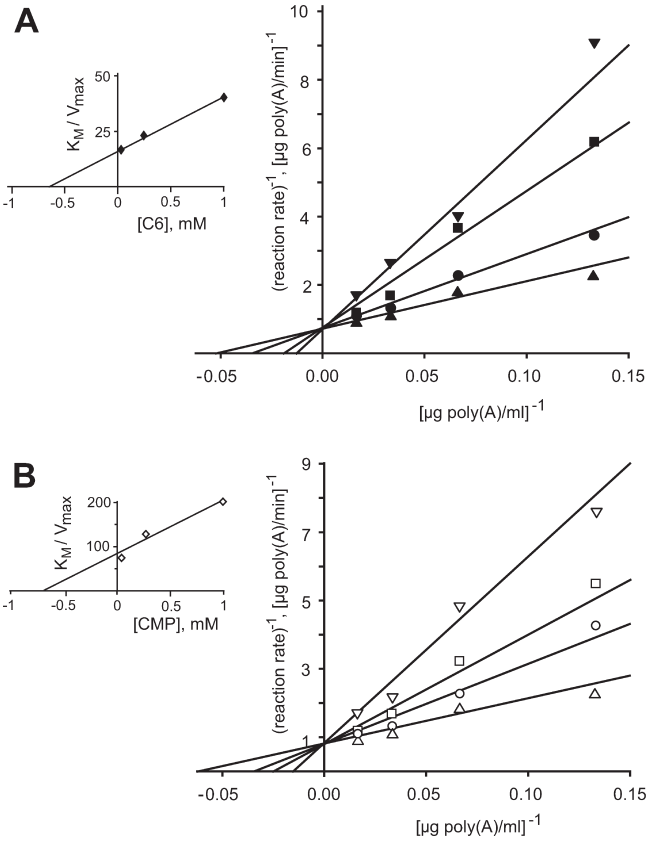

FIGURE 3: C6 and CMP are noncompetitive inhibitors of PARN. Double reciprocal plots $1/v$ versus 1/[substrate] for PARN activity in the presence of C6 (filled markers in A) or CMP (empty markers in B) are shown. The C6 concentrations (filled markers in A) and CMP concentrations (empty markers in B) were 0 mM (triangle), 0.025 mM (circle), 0.25 mM (square), and 1 mM (inverted triangle). Representative plots of at least three independent experiments are shown. Insets: slopes (K_M/V_{max}) of the double reciprocal lines versus the nucleotide concentrations.

Mg(II) Ions Do Not Release Inhibition by A2, A6, and C6. Previous studies have shown that Mg(II) ions are important for PARN activity, although no such ions were found in the crystal structure of a truncated but active form of PARN (*7*, *8*). In addition, in our previous report we observed that increased Mg(II) ion concentrations could reverse the inhibition by natural di- and triphosphate nucleotides but not the inhibition by monophosphate nucleotides (*19*). Therefore, we wanted to exclude the possibility that the observed inhibition of PARN by the synthetic nucleosides could, somehow, be rescued using excess Mg(II), although these nucleotides do not include any phosphate group. We performed deadenylation assays with Mg(II) concentrations varying below (10-fold) and above (10-fold) the concentration of the standard assay conditions. Interestingly, under the conditions tested, Mg(II) concentration could not reverse the inhibitory effect of A2, A6, and C6 (Figure 4). These data show that the effect of the novel synthetic compounds is independent of the local Mg(II) concentration and that the inhibitory effect of these compounds cannot be deprived by altering Mg(II) levels.

Prediction of C6, A6, and A2 Docking in the Active Site of PARN. To further analyze the specific interactions of C6, A6, and A2 fluoro-pyranosyl nucleosides with PARN, we performed molecular docking experiments *in-silico* using the known crystal structure of PARN (*8*) as the receptor. The lowest energy MOE-docked conformations for the compounds under study are shown in Figure 5. All docking conformations of C6 form a single cluster

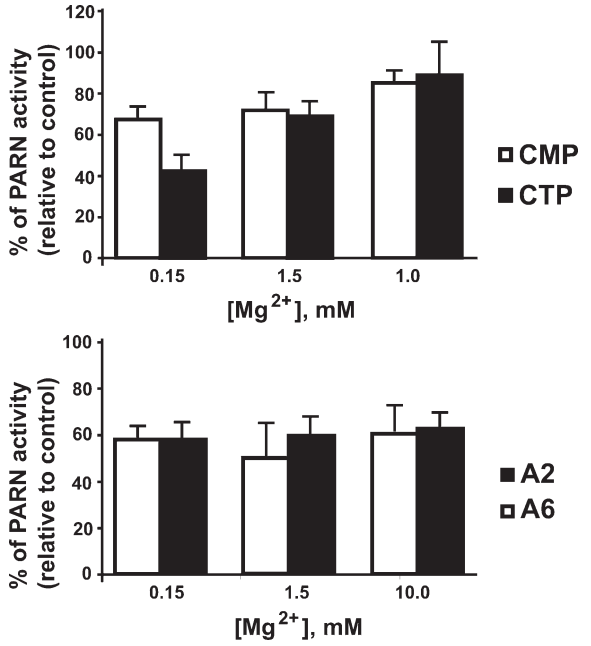

FIGURE 4: Effect of Mg(II) in the inhibition of PARN by purine nucleotides. (Top) Relative activity inhibition by 1 mM A2 (empty bars) or 1 mM A6 (filled bars) in the presence of 0, 1.5, and 15 mM Mg (II). (Bottom) Relative activity in the presence of 1 mM C6 (empty bars) or 1 mM CMP (filled bars) in the presence of 0, 1.5, and 10 mM Mg(II). The results are the mean values from at least three independent experiments.

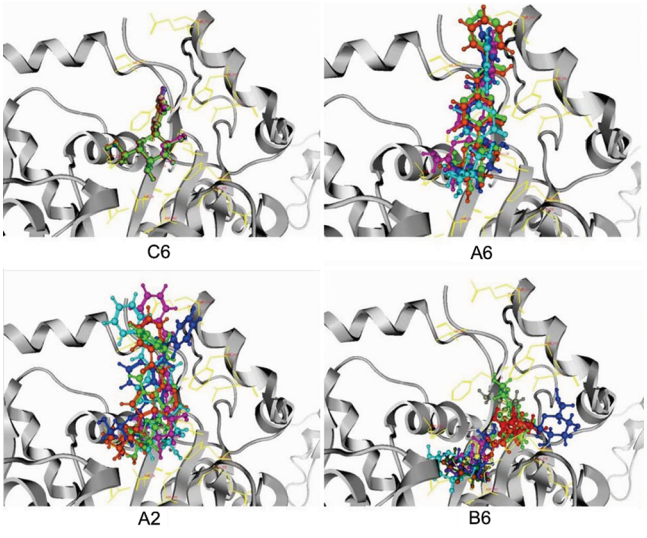

FIGURE 5: Docking of compounds C6, A6, A2, and B6 in the PARN active site. The lower energy and most prevalent docked conformations of compounds A2, A6, C6, and B6 in PARN. Clustering of docking conformations suggests a high binding efficiency of the C6 and A6 compounds. The A2 docking conformations exhibit a lower degree of clustering. The scattering of the B6 docking conformations implies a nonconsensus binding mode of this compound.

falling within a max rmsd range < 0.1 Å, suggesting a high specificity of this compound for the given receptor (Figure 5). The establishment of a hydrogen bond between the 5′ sugar -OH and Glu30, optimizes the geometry of the other two -OH groups of the sugar ring to donate electrons to two Asp residues (Asp382 and Asp28) of the catalytic triad (Figure 6).

Concerning A6, at least 6 out of 10 total docking conformations gave results that fall within a single cluster indicating that there is a preferred binding orientation for compound A6

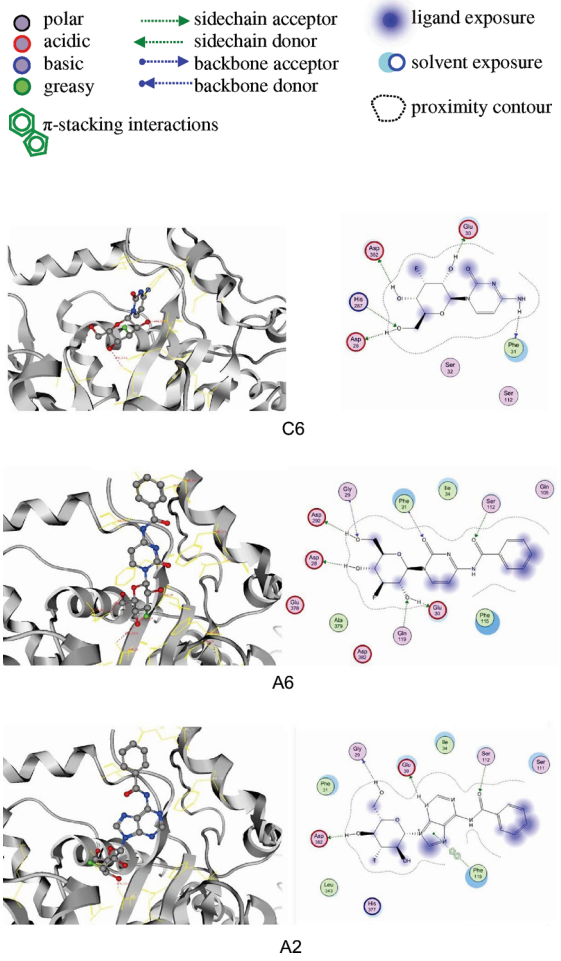

FIGURE 6: Interactions of PARN with compounds C6, A6, and A2. Left: 3D models of the binding mode of the compounds C6, A6, and A2 in the PARN active site. Right: Ligplot interaction maps for each compound. Interactions are drawn according to the table located above the figure.

(Figure 5). Molecular dynamics simulations were subsequently performed in order to validate the docking results. The MD simulations confirmed the binding orientation of A6, which is optimal for allowing the -OH groups of the sugar ring to establish H-bonding (Asp28 and Asp292) and hydrophobic (Asp382) interactions with the Asp residues of the catalytic triad (Figure 6). Similar to compound C6, the 5′-OH hydrogen bonds to Glu30. The critical role of the -OH groups at positions 2′, 4′, and 6′ is also supported by the fact that compound A5, which bears the less polar acetyl groups in these positions, is less hydrophilic and does not inhibit PARN activity (data not shown). The presence of the extra phenyl ring (Bz group) in A6 compared to C6 seems to have further optimized the interaction with the receptor via hydrophobic interactions of the phenyl ring, allowing for an optimal orientation of the sugar ring to interact with the catalytic Asp residues (Figure 6). In addition, the cytosine heterocyclic aromatic ring adopts an optimal geometry establishing hydrophobic interactions with two phenyl rings of the receptor (Phe31 and Phe115).

However, the more complex adenosine rings of compound A2 setup a very highly conjugated system in the middle of the compound establishing pi-stacking interactions with the receptor (Phe115) as shown in Figure 6. The five-membered ring of the adenosine moiety interacts with Phe115, rather than the phenyl ring in the case of the cytosine-based compound. As a result, the

lowest energy docking conformation of the A2 compound is tilted, slightly offset, not allowing the 5′-OH to Glu30 hydrogen bonding, and consequently the interaction of the sugar -OH groups with the Asp residues of the catalytic triad (Figure 6).

To compare the *in silico* behavior of the inhibitory compounds with the other molecules that were tested, we performed simulations for every synthetic nucleoside. However, it was evident from our analysis that the bulkier compounds (such as A1, A5, and A7, Figure 1) could not fit in the docking models that we attempted to produce (data not shown). Therefore, we concluded that since B6 represents the structural base for the subsequent synthesis of the compounds tested, it was used as the control compound. Docking of compound B6 showed that the sugar moiety of A6 alone is incapable of establishing H-bonding with the catalytic triad as indicated by the scattering of the docking conformations of B6 in the active site of the enzyme (Figure 5).

Taken together, these data suggest that the aromatic rings of the adenosine-based A2 compound constitute a bulky and highly conjugated core that reduces its inhibitory potency when compared to the cytosine-based compounds C6 and A6. The contribution of the extra phenyl ring of compound A6 further improves its binding mode, making it a more potent inhibitor of PARN. Finally, both our *in vitro* and *in silico* analyses suggest that human PARN could represent a new molecular target for these compounds *in vivo* and that these analogues could serve as lead compounds for the development of novel inhibitors of PARN with potential therapeutic use.

DISCUSSION

In our search for competitive PARN inhibitors with possible therapeutic potential, we studied the effect of a novel class of nucleoside analogues, the fluoro-pyranosyl nucleosides. Nucleoside analogues have been widely explored as potential antitumor and antiviral therapeutic agents. Modifications on the base, the sugar moiety, or both have been used in order to improve their therapeutic index mainly by targeting key enzymes. Human PARN represents a potential target for drug development that has not been extensively studied so far.

The sugar component of the nucleosides that were chosen for the present study is composed of an uncommon six-membered ring, a modification that has been well associated with anticancer and immunosuppressive effects (*23*, *29*, *30*). The fluorine atom that they carry in their sugar moiety improves activity, lipophilicity, and cell membrane penetration (*36*−*39*). Additionally, modifications with the benzoyl group (Bz) have been used in nucleoside synthesis; dATP analogues that bear a Bz-modified adenine have been recognized and incorporated into DNA by a Klenow fragment of DNA polymerase I (*40*). Bz also has been used in compounds to inhibit the RNase H domain of HIV RT (*26*). All these features have established fluoro-pyranosyl nucleosides as promising compounds for drug development. Two of the benzoyl fluoro-pyranosyl nucleosides tested in this work (A2 and A6) behave as competitive inhibitors of the enzyme and carry either Bz-modified adenine (A2) or Bz-modified cytosine (A6) as the base group (Figure 1). The K_i values for these compounds were found to be significantly lower compared to those of natural nucleotides AMP and CMP that also exhibit competitive inhibition (Figure 4, Table 1). The compound C6, which carries a modified sugar moiety but no Bz-modified base (cytidine), could also inhibit PARN in a competitive manner with K_i = 0.65 mM, a value comparable to that of the closest structurally similar natural nucleotide such as CMP. Comparing the K_i values of A6, C6, and the structurally similar natural nucleotide CMP that all bear cytosine as the base (0.21, 0.65, and 0.72 mM, respectively), it is evident that benzoyl modification is crucial for more efficient inhibition. This could probably be attributed to the fact that the structure of the group helps the nucleoside to fit better in the active site and that its charge stabilizes the interaction with the critical catalytic amino acids. Finally, the initiatory compound B6 showed no consensus in the biding mode for the active site of the enzyme and no inhibitory effect on enzymatic activity, an observation that was also verified by the *in vitro* biochemical analysis (data not shown).

To acquire information on how C6, A6, and A2 interact with the active site of PARN and support the biochemical data, we performed MD simulations. Our results show that all three compounds could be accommodated into the active site of the enzyme, thus favoring effective suppression of its activity through specific interactions. A2 could inhibit PARN competitively, but no inhibition was observed when the -OH groups on the sugar were replaced with acetyl or the even bulkier trityl groups (compounds A1, A3, and A4). This inefficacy can be attributed probably to the different chemical behavior and the bulkier acetyl groups that do not fit properly into the catalytic pocket. Analogous observations were made for A6 suggesting a crucial role for the hydroxyl groups on the sugar moiety. Furthermore, the presence of the benzoyl group improved the inhibitory effect of the cytosine base, as reflected by the K_i values of compounds A2 and A6 compared to that of C6 (Table 1). Our data suggests that the bulky and conjugated core formed by the aromatic rings of A2 reduces its inhibitory potency when compared to that of the cytosine-based compounds. However, the contribution of the extra phenyl ring of compound A6 compared to that of C6 further improves its binding affinity, making it a more potent inhibitor of PARN.

The *in silico* analysis presented in this work shows the important interactions between the sugar moiety and the main catalytic amino acids, as also observed experimentally in the poly (A)-bound form of PARN (*8*). The optimal binding orientation of C6 in the active site is the one that allows the -OH groups of the sugar ring to establish H-bonding interactions with the three catalytic Asp residues (Figure 6) and for enhanced hydrophobic interactions between the six-memeberd sugar ring and the receptor. The addition of an extra phenyl moiety (compound A6) enhances the interactions with the active site of the receptor (Figure 6). Taken together with the K_i values for A2, A6, C6, AMP, and CMP, our data show that at least in the case of modified nucleosides tested here, PARN has a higher affinity for cytosine rather than adenine-based compounds. Although PARN distinguishes poly(A) from poly(U) and cannot degrade poly(C) or poly(G) (*6*, *13*), it seems that, at least in the case of modified nucleosides tested, it binds better a cytosine than an adenine. It should be noted that substrate recognition by PARN remains an unresolved issue and an important observation is that despite the fact that the enzyme degrades poly(A) efficiently, there are no specific hydrogen-bonding interactions between the adenine bases and the enzyme (*8*).

The involvement of Mg(II) ions in deadenylation reactions in the presence of the analogues has also been studied. We have previously shown that the inhibitory effect of purine nucleotides with three phosphate groups (ATP and GTP) or two phosphate groups (ADP and GDP) could be released when Mg(II) concentration is increased but not that of nucleotides with one

phosphate group (AMP and GMP). Our results, are in accordance with these observations and show that the elevated presence of Mg(II) did not affect the inhibition of PARN by the modified nucleosides (Figure 4) possibly due to the lack of any phosphate groups. Several studies debate on the binding mode of Mg(II) ions to phosphate groups. It has been reported that Mg(II) binds only the β-phosphate of ATP, that Mg-ATP is a β,γ-bidentate or a mixture of α, β-, β, γ-, and α,γ-bidentates, and finally that the metal interacts with α- and β-phosphates of ADP and all phosphates of ATP (*41*−*44*). The actual presence of Mg(II) in the active site of PARN that actively participates in the mechanism has been explored in detail (*7*). In that report, a schematic drawing of the proposed two-metal ion mechanism for PARN was based on a previous report from the same group (*45*) suggesting that the PARN active site resembles the 3′-5′ exonuclease active site of DNA pol I. The authors suggested that three aspartic acid residues (D28, D292, and D382) and one glutamic acid (E30) residue coordinate two metal ions either directly or indirectly via bridging water molecules. However, Mg(II) could be substituted by other divalent metal ions (such as Mn^{2+} or Co^{2+}), raising questions on the absolute requirement for Mg^{2+} *per se* for the catalytic mechanism. Furthermore, it has been reported that Mg(II) ions release the inhibition of PARN and Klenow fragment of DNA polymerase activity by neomycin B, which behaves as a mixed noncompetitive inhibitor (*17*). In that report, the authors show that the K_i of neomycin B for PARN is independent of the concentration of Mg(II) ions and suggest that neomycin B and divalent ions compete for the same site or for overlapping binding sites (*17*). It is also known that Mg(II) binds weakly to proteins with $K_a \leq 10^5$ M^{-1}, where in the case of exoribonucleases, such as the Klenow fragment of DNA polymerase, both single- and two-metal-ion mechanisms have been proposed (*46*). Thus, the inability of Mg(II) to release the inhibition of PARN could attributed either to the weak affinity of the metal for the enzyme or to overlapping binding sites (for the metal and the inhibitor). As mentioned above (*8*), the crystal structure of a C-terminal truncated human PARN was determined in two states (free and RNA-bound forms), but interestingly, the authors reported that they failed to observe the presence of metal ions in the active site in the ligand-free form of PARN, although Mg(II) was included in the crystallization conditions (in the same order of magnitude as that used in standard deadenlyation assays, i.e., between 1.5 and 2 mM). In the same report, the crystallographic data showed that the essential amino acids for PARN activity, i.e., (D28, D282, D382, and E30) preferably interact with either the ribose or the phosphate group of an oligo (A) substrate, while biochemical data showed that H377 is also essential for catalytic activity and interacts with the phosphate group. In our analysis, the same amino acids are involved in the coordination of the sugar moiety of the nucleosides in the active site. Furthermore, the fact that increased Mg(II) can indeed release the inhibition of PARN activity by purine tri- and diphosphate nucleotides (RTP and RDP) but not by monophosphate nucleotides (RMP) suggests an inhibition mode that is probably independent of the metal ion presence. Moreover, in a recent report (*47*) where the effect of Mg(II) on thermal stability of PARN was examined the enzyme could function, albeit slower, even in the absence of Mg(II). Although Mg(II) is necessary for the overall PARN functional integrity, the above-mentioned data could explain why in our study the increased Mg(II) concentration did not influence the inhibition level of the nucleoside analogues. Furthermore, a very recent study on the structural basis of cap binding to PARN, revealed that cap binding and active site domains partially overlap (*48*). Interestingly, a common aspartate residue (D28) that appears to be involved in the coordination of the 4′-OH group of A2, A6, and C6 in our study and possibly in the Mg^{2+} coordination also appears as the common residue between the cap-binding domain and the active site domain. In the present study, it is evident that the interaction of the nucleoside analogues did not interfere with the necessary Mg(II), a feature that is essential for the effectiveness of these analogues as potential therapeutic compounds in the cellular environment.

The present study suggests that PARN represents at least one of the keto-pyranosyl analogues' targets at the molecular level. From this point of view, these analogues could exert their effect by interfering with the mRNA lifecycle where PARN is a key player. Further development of similar compounds that target mRNA turnover factors could be used for more in-depth biochemical studies and eventually for therapeutic applications. This suggestion is supported by the documented anticancer and antiviral potency that these compounds exhibit in cell cultures.

SUPPORTING INFORMATION AVAILABLE

Deadenylation rate as a function of time in the presence or absence of inhibitors. This material is available free of charge via the Internet at http://pubs.acs.org.

REFERENCES

(1) Goldstrohm, A. C., and Wickens, M. (2008) Multifunctional deadenylase complexes diversify mRNA control. *Nat. Rev. Mol. Cell Biol. 9*, 337–344.
(2) Dehlin, E., Wormington, M., Korner, C. G., and Wahle, E. (2000) Cap-dependent deadenylation of mRNA. *EMBO J. 19*, 1079–1086.
(3) Gao, M., Wilusz, C. J., Peltz, S. W., and Wilusz, J. (2001) A novel mRNA-decapping activity in HeLa cytoplasmic extracts is regulated by AU-rich elements. *EMBO J. 20*, 1134–1143.
(4) Martinez, J., Ren, Y. G., Nilsson, P., Ehrenberg, M., and Virtanen, A. (2001) The mRNA cap structure stimulates rate of poly(A) removal and amplifies processivity of degradation. *J. Biol. Chem. 276*, 27923–27929.
(5) Opyrchal, M., Anderson, J. R., Sokoloski, K. J., Wilusz, C. J., and Wilusz, J. (2005) A cell-free mRNA stability assay reveals conservation of the enzymes and mechanisms of mRNA decay between mosquito and mammalian cell lines. *Insect Biochem. Mol. Biol. 35*, 1321–1334.
(6) Korner, C. G., and Wahle, E. (1997) Poly(A) tail shortening by a mammalian poly(A)-specific 3′-exoribonuclease. *J. Biol. Chem. 272*, 10448–10456.
(7) Ren, Y. G., Kirsebom, L. A., and Virtanen, A. (2004) Coordination of divalent metal ions in the active site of poly(A)-specific ribonuclease. *J. Biol. Chem. 279*, 48702–48706.
(8) Wu, M., Reuter, M., Lilie, H., Liu, Y., Wahle, E., and Song, H. (2005) Structural insight into poly(A) binding and catalytic mechanism of human PARN. *EMBO J. 24*, 4082–4093.
(9) Balatsos, N. A., Nilsson, P., Mazza, C., Cusack, S., and Virtanen, A. (2006) Inhibition of mRNA deadenylation by the nuclear cap binding complex (CBC). *J. Biol. Chem. 281*, 4517–4522.
(10) Gao, M., Fritz, D. T., Ford, L. P., and Wilusz, J. (2000) Interaction between a poly(A)-specific ribonuclease and the 5′ cap influences mRNA deadenylation rates in vitro. *Mol. Cell 5*, 479–488.
(11) Gherzi, R., Lee, K. Y., Briata, P., Wegmuller, D., Moroni, C., Karin, M., and Chen, C. Y. (2004) A KH domain RNA binding protein, KSRP, promotes ARE-directed mRNA turnover by recruiting the degradation machinery. *Mol. Cell 14*, 571–583.
(12) Lai, W. S., Kennington, E. A., and Blackshear, P. J. (2003) Tristetraprolin and its family members can promote the cell-free deadenylation of AU-rich element-containing mRNAs by poly(A) ribonuclease. *Mol. Cell. Biol. 23*, 3798–3812.
(13) Martinez, J., Ren, Y. G., Thuresson, A. C., Hellman, U., Astrom, J., and Virtanen, A. (2000) A 54-kDa fragment of the Poly(A)-specific ribonuclease is an oligomeric, processive, and cap-interacting Poly (A)-specific 3′ exonuclease. *J. Biol. Chem. 275*, 24222–24230.

(14) Seal, R., Temperley, R., Wilusz, J., Lightowlers, R. N., and Chrzanowska-Lightowlers, Z. M. (2005) Serum-deprivation stimulates cap-binding by PARN at the expense of eIF4E, consistent with the observed decrease in mRNA stability. *Nucleic Acids Res. 33*, 376–387.
(15) Tran, H., Schilling, M., Wirbelauer, C., Hess, D., and Nagamine, Y. (2004) Facilitation of mRNA deadenylation and decay by the exosome-bound, DExH protein RHAU. *Mol. Cell 13*, 101–111.
(16) Moraes, K. C., Wilusz, C. J., and Wilusz, J. (2006) CUG-BP binds to RNA substrates and recruits PARN deadenylase. *RNA 12*, 1084–1091.
(17) Ren, Y. G., Martinez, J., Kirsebom, L. A., and Virtanen, A. (2002) Inhibition of Klenow DNA polymerase and poly(A)-specific ribonuclease by aminoglycosides. *RNA 8*, 1393–1400.
(18) Astrom, J., Astrom, A., and Virtanen, A. (1992) Properties of a HeLa cell 3′ exonuclease specific for degrading poly(A) tails of mammalian mRNA. *J. Biol. Chem. 267*, 18154–18159.
(19) Balatsos, N. A., Anastasakis, D., and Stathopoulos, C. (2009) Inhibition of human poly(A)-specific ribonuclease (PARN) by purine nucleotides: kinetic analysis. *J. Enzyme Inhib. Med. Chem. 24*, 516–523.
(20) Meng, W. D., and Qing, F. L. (2006) Fluorinated nucleosides as antiviral and antitumor agents. *Curr. Top. Med. Chem. 6*, 1499–1528.
(21) Gmeiner, W. H. (2002) Antimetabolite incorporation into DNA: structural and thermodynamic basis for anticancer activity. *Biopolymers 65*, 180–189.
(22) Lopez, C., Watanabe, K. A., and Fox, J. J. (1980) 2′-fluoro-5-iodoaracytosine, a potent and selective anti-herpesvirus agent. *Antimicrob. Agents Chemother. 17*, 803–806.
(23) Plunkett, W., Huang, P., Searcy, C. E., and Gandhi, V. (1996) Gemcitabine: preclinical pharmacology and mechanisms of action. *Semin. Oncol. 23*, 3–15.
(24) Vivet-Boudou, V., Didierjean, J., Isel, C., and Marquet, R. (2006) Nucleoside and nucleotide inhibitors of HIV-1 replication. *Cell. Mol. Life Sci. 63*, 163–186.
(25) Warwick, Z., and Churchill, D. (2008) Nucleoside analogues in 2008. *J. HIV Ther. 13*, 3–8.
(26) Himmel, D. M., Sarafianos, S. G., Dharmasena, S., Hossain, M. M., McCoy-Simandle, K., Ilina, T., Clark, A. D. Jr., Knight, J. L., Julias, J. G., Clark, P. K., Krogh-Jespersen, K., Levy, R. M., Hughes, S. H., Parniak, M. A., and Arnold, E. (2006) HIV-1 reverse transcriptase structure with RNase H inhibitor dihydroxy benzoyl naphthyl hydrazone bound at a novel site. *ACS Chem. Biol. 1*, 702–712.
(27) Nikolenko, G. N., Palmer, S., Maldarelli, F., Mellors, J. W., Coffin, J. M., and Pathak, V. K. (2005) Mechanism for nucleoside analog-mediated abrogation of HIV-1 replication: balance between RNase H activity and nucleotide excision. *Proc. Natl. Acad. Sci. U.S.A. 102*, 2093–2098.
(28) Roquebert, B., and Marcelin, A. G. (2008) The involvement of HIV-1 RNase H in resistance to nucleoside analogues. *J. Antimicrob. Chemother. 61*, 973–975.
(29) Alaoui-Jamali, M. A., Lasne, C., Antonakis, K., and Chouroulinkov, I. (1986) Absence of genotoxic effects in cells exposed to four ketonucleoside derivatives. *Mutagenesis 1*, 411–417.
(30) Alaoui-Jamali, M. A., Tapiero, H., Antonakis, K., and Chouroulinkov, I. (1987) Cytotoxic potential of ketonucleosides. *Anticancer Res. 7*, 501–504.
(31) Manta, S., Agelis, G., Botic, T., Cencic, A., and Komiotis, D. (2008) Unsaturated fluoro-ketopyranosyl nucleosides: synthesis and biological evaluation of 3-fluoro-4-keto-beta-D-glucopyranosyl derivatives of N(4)-benzoyl cytosine and N(6)-benzoyl adenine. *Eur. J. Med. Chem. 43*, 420–428.
(32) Paterson, J., Uriel, C., Egron, M. J., Herscovici, J., Antonakis, K., and Alaoui-Jamali, M. A. (1998) Antiproliferative and apoptotic activities of ketonucleosides and keto-C-glycosides against non-small-cell lung cancer cells with intrinsic drug resistance. *Antimicrob. Agents Chemother. 42*, 779–784.
(33) Nilsson, P., and Virtanen, A. (2006) Expression and purification of recombinant poly(A)-specific ribonuclease (PARN). *Int. J. Biol. Macromol. 39*, 95–99.
(34) Cheng, Y., Liu, W. F., Yan, Y. B., and Zhou, H. M. (2006) A nonradioactive assay for poly(a)-specific ribonuclease activity by methylene blue colorimetry. *Protein Pept. Lett. 13*, 125–128.
(35) MOE , C. C. G., Montreal, Canada.
(36) Blandin, M., Tran Dinh, S., Catlin, J. C., and Guschlbauer, W. (1974) Nucleoside conformations. 16. Nuclear magnetic resonance and circular dichroism studies on pyrimidine-2′-fluoro-2′-deoxyribonucleosides. *Biochim. Biophys. Acta 361*, 249–256.
(37) Lipnick, R. L., and Fissekis, J. D. (1980) A comparative conformational study of certain 2′-deoxy-2′-fluoro-arabinofuranosylcytosine nucleosides. *Biochim. Biophys. Acta 608*, 96–102.
(38) Morton, G. O., Lancaster, J. E., Van Lear, G. E., Fulmor, W., and Meyer, W. E. (1969) The structure of nucleocidin. 3. (A new structure). *J. Am. Chem. Soc. 91*, 1535–1537.
(39) Van Aerschot, A., Herdewijn, P., Balzarini, J., Pauwels, R., and De Clercq, E. (1989) 3′-Fluoro-2′,3′-dideoxy-5-chlorouridine: most selective anti-HIV-1 agent among a series of new 2′- and 3′-fluorinated 2′,3′-dideoxynucleoside analogues. *J. Med. Chem. 32*, 1743–1749.
(40) Zofall, M., and Bartholomew, B. (2000) Two novel dATP analogs for DNA photoaffinity labeling. *Nucleic Acids Res. 28*, 4382–4390.
(41) Cohn, M., and Hughes, T. R. Jr. (1962) Nuclear magnetic resonance spectra of adenosine di- and triphosphate. II. Effect of complexing with divalent metal ions. *J. Biol. Chem. 237*, 176–181.
(42) Huang, S. L., and Tsai, M. D. (1982) Does the magnesium(II) ion interact with the alpha-phosphate of adenosine triphosphate? An investigation by oxygen-17 nuclear magnetic resonance. *Biochemistry 21*, 951–959.
(43) Ramirez, F., and Marecek, J. F. (1980) Coordination of magnesium with adenosine 5′-diphosphate and triphosphate. *Biochim. Biophys. Acta 589*, 21–29.
(44) Son, T. D., Roux, M., and Ellenberger, M. (1975) Interaction of Mg2+ ions with nucleoside triphosphates by phosphorus magnetic resonance spectroscopy. *Nucleic Acids Res. 2*, 1101–1110.
(45) Ren, Y. G., Martinez, J., and Virtanen, A. (2002) Identification of the active site of poly(A)-specific ribonuclease by site-directed mutagenesis and Fe(2+)-mediated cleavage. *J. Biol. Chem. 277*, 5982–5987.
(46) Cowan, J. A. (2002) Structural and catalytic chemistry of magnesium-dependent enzymes. *Biometals 15*, 225–235.
(47) Liu, W. F., Zhang, A., Cheng, Y., Zhou, H. M., and Yan, Y. B. (2007) Effect of magnesium ions on the thermal stability of human poly(A)-specific ribonuclease. *FEBS Lett. 581*, 1047–1052.
(48) Wu, M., Nilsson, P., Henriksson, N., Niedzwiecka, A., Lim, M. K., Cheng, Z., Kokkoris, K., Virtanen, A., and Song, H. (2009) Structural basis of m(7)GpppG binding to poly(A)-specific ribonuclease. *Structure 17*, 276–286.